



## $\pi$ -extended phosphepines: redox and optically active P-heterocycles with non-planar framework

Thomas Delouche, Anabella Mocanu, Thierry Roisnel, Rózsa Szűcs,  
Emmanuel Jacques, Zoltán Benkő, László Nyulászi, Pierre-Antoine Bouit,  
Muriel Hissler

### ► To cite this version:

Thomas Delouche, Anabella Mocanu, Thierry Roisnel, Rózsa Szűcs, Emmanuel Jacques, et al..  $\pi$ -extended phosphepines: redox and optically active P-heterocycles with non-planar framework. Organic Letters, 2019, 21 (3), pp.802-806. 10.1021/acs.orglett.8b04064 . hal-01992161

**HAL Id: hal-01992161**

**<https://hal.science/hal-01992161>**

Submitted on 24 Jan 2019

**HAL** is a multi-disciplinary open access archive for the deposit and dissemination of scientific research documents, whether they are published or not. The documents may come from teaching and research institutions in France or abroad, or from public or private research centers.

L'archive ouverte pluridisciplinaire **HAL**, est destinée au dépôt et à la diffusion de documents scientifiques de niveau recherche, publiés ou non, émanant des établissements d'enseignement et de recherche français ou étrangers, des laboratoires publics ou privés.

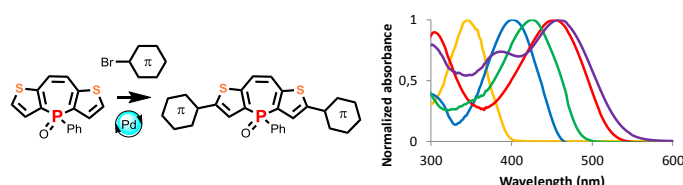
# $\pi$ -extended phosphepines: redox and optically active P-heterocycles with non-planar framework

Thomas Delouche,<sup>†</sup> Anabella Mocanu,<sup>†</sup> Thierry Roisnel,<sup>†</sup> Rózsa Szűcs,<sup>‡</sup> Emmanuel Jacques,<sup>§</sup> Zoltán Benkő,<sup>‡\*</sup> László Nyulászi,<sup>‡\*</sup> Pierre-Antoine Bouit,<sup>†\*</sup> Muriel Hissler<sup>†\*</sup>

<sup>†</sup> Univ Rennes, CNRS, ISCR - UMR 6226, ScanMAT - UMS 2001, F-35000 Rennes.

<sup>§</sup> Univ Rennes, CNRS, IETR - UMR 6164, F-35000 Rennes, France

<sup>‡</sup> Department of Inorganic and Analytical Chemistry, Budapest University of Technology and Economics, and MTA-BME Computation Driven Chemistry Research Group. Szt. Gellert ter 4 H-1111 Budapest, Hungary



**ABSTRACT:** In this letter, we present the synthesis of a new family of  $\pi$ -extended dithieno[*b,f*]phosphepines. The Pd-catalyzed direct-arylation allows the introduction of various substituents, which tune the absorption/emission in the visible range as well as the redox properties. All those modifications were rationalized through DFT calculations. The physical properties of ambipolar phosphepine with diphenylamino substituents conduct us to use it as a semi-conductor in a p-type organic field-effect transistors (OFETs).

In the past decade,  $\pi$ -conjugated systems based on heterocycles have been widely studied following the first reports on their successful incorporation in (opto)-electronic devices (organic photovoltaics (OPV), organic field-effect transistors (OFETs), organic light-emitting diodes (OLEDs)).<sup>1</sup> While the initial structures mainly incorporate thiophene rings,<sup>2</sup> more and more heterocycles with O, N, B, Si... have been used as building blocks.<sup>3</sup> Among them, phosphorus-based heterocycles are interesting as their reactivities and physico-chemical properties highly depend on the P-atom's substituents as well as the nature of the heterocycle in which it is embedded.<sup>4</sup> Thanks to the richness of the organophosphorus chemistry, plethora of P-heterocycles have been developed such as 4-membered (phosphetenes),<sup>5</sup> 5-membered (phospholes),<sup>6</sup> 6-membered (such as phosphinines)<sup>7</sup> or 7-membered rings (phosphepines).<sup>8</sup> The most widely used P-based building block for the construction of  $\pi$ -conjugated systems for (opto)-electronics is the phosphole ring.<sup>6a</sup> The corresponding phosphole-based semiconductors have been successfully inserted into OLEDs, OPV or organic batteries.<sup>6,9</sup> So far, only few examples of optically/redox-active phosphepine based  $\pi$ -conjugated systems have been described (A-D, Figure 1).<sup>8</sup> The  $\pi$ -delocalization of the ring as well as its conformational flexibility make the phosphepine a singular  $\pi$ -synthon compared to phospholes. This prompted us to search for an alternative synthetic approach to develop  $\pi$ -extended optically and redox-active phosphepines.

In this letter, we present the synthesis of a new family of dithieno[*b,f*]phosphepine-based  $\pi$ -system (Scheme 1) accessed by Pd-catalyzed direct-arylation. The optical and redox properties and the electronic structure of these compounds are reported and a selected compound is used as p-semiconductor in OFET.

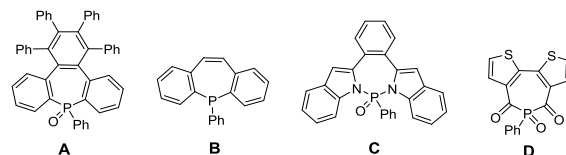
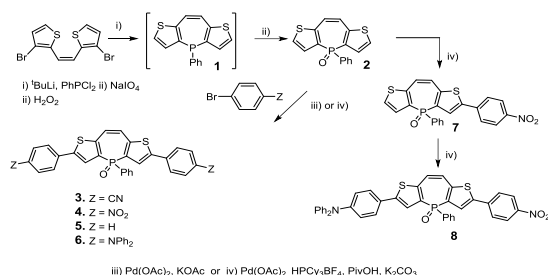


Figure 1. Reported optically/redox-active phosphepines A-D.

Dithieno[*b,f*]phosphepine **1** (Scheme 1) was synthesized by adapting the synthetic approach developed by Tovar *et al.* for the preparation of thiophene-fused borepines.<sup>10,11</sup> Dibromodithienylethene was subsequently treated with 2 equivalents of *t*-BuLi and one equivalent of  $\text{PhPCl}_2$  at  $-78^\circ\text{C}$  affording compound **1** (Scheme 1) ( $^{31}\text{P}$  NMR:  $\delta = -46.4$  ppm). Since the P-atom retains its phosphine-like reactivity, this air sensitive compound **1** was directly oxidized into compound **2** ( $^{31}\text{P}$  NMR:  $+11.7$  ppm). Then, compound **2** was used as a key starting material for the preparation of  $\pi$ -extended phosphepines because thiophenes are ideal synthons for Pd-catalyzed direct-arylation.<sup>12</sup> The reaction between **2** and 4-cyano-bromobenzene or 4-nitro-bromobenzene proceeds nicely under “classical” direct arylation conditions (5%  $\text{Pd}(\text{OAc})_2$  as catalyst, KOAc as base) in DMAc at  $140^\circ\text{C}$  to afford **3** and **4** (Scheme 1) in good yields (58% and 66%, respectively). However, in order to introduce an electron-rich substituent, the catalytic conditions have been changed:  $\text{K}_2\text{CO}_3$  was used as base, with the addition of  $\text{HPCy}_3\text{BF}_4$  (ligand) and PivOH.<sup>13,14</sup> Using this synthetic methodology, a novel family of symmetrical  $\pi$ -extended phosphepines featuring electron-withdrawing (**3-4**, Scheme 2) or electron-donating end-groups (**5-6**) could be prepared in good yields (56-66%). Using a sequential approach, the asymmetric compound **8** was prepared by the successive insertion of nitrophenyl and diphenylaminophenyl substituents using our previously optimized catalytic conditions. All

compounds **2-8** were characterized by multinuclear NMR and high-resolution mass spectrometry (HR-MS).

Scheme 1. Synthesis of  $\pi$ -extended dithieno[*b,f*]phosphepine **1-8**.



Additionally, compounds **2-6** were characterized by single crystal X-ray diffraction (Figure 2 and Table S1). In all five compounds, the seven membered rings present non-planar boat-like conformation. While in compounds **2**, **4** and **5** the phenyl substituents on the P-atom are in equatorial position, and are (almost) perpendicular to the phosphepine ring, in case of **3** and **6** the axially oriented phenyl moiety is parallel to the vinylic bond of the seven-membered ring as is shown in Figure 2, Figure S1-S6 and Table S2. Noteworthy, calculations conducted with the B3LYP, CAM-B3LYP and M06-2X methods suggest that the lowest energy conformer is the one with perpendicular phenyl in each case. Furthermore, the bond lengths within the seven membered rings are quite similar for all the compounds reported here and also compare well with those of compound **B**,<sup>Erreur ! Signet non défini.a</sup> indicating an alternation of double and single bonds (Figure 2, Table S2). The possible conformations (Figure 2) were studied with DFT calculations with different functionals. The energy difference of the three calculated conformers did not exceed 1 kcal/mol (Table S3-4, S6-7), furthermore, the interconversion barrier for **2** was under 2.6 kcal/mol) for all tested methods, indicating a virtually free interconversion at RT in the gaseous phase (Table S7). This low barrier is supported by the variable temperature <sup>31</sup>P and <sup>1</sup>H NMR experiments (300-223°K - CDCl<sub>3</sub>) on compound **2** as no coalescence could be reached (Figure S10).<sup>Erreur ! Signet non défini.a</sup> The solid state organization of the different compounds shows no clear intermolecular interactions. However, the crystal packing probably influences these flexible frameworks to favor one conformer over the other due to the low barrier for interconversion.

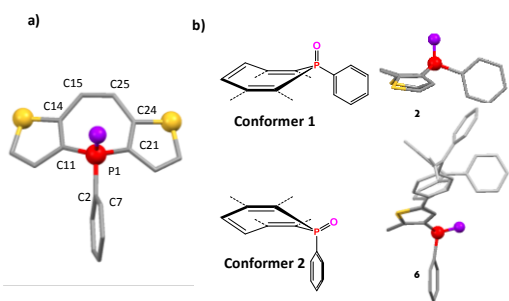


Figure 2. a) X-ray structure of **2** (top and side-view, a-b). hydrogen atoms are omitted for clarity Selected bond lengths (Å), bond angles (deg), and torsion angles (deg) are as follows. **2**: P1–C11 = 1.7880(15), P1–C21 = 1.7825(16), P1–C2 = 1.8014(16), C11–C14 = 1.390(2), C14–C15 = 1.445(2), C15–C25 = 1.350(2); C11–P1–C21 = 104.21(7), C11–P1–C2 = 106.95(7), C21–P1–C2 = 104.93(7); C7–C2–P1–C21 = -60.73(14). b) view of the 2 conformers illustrated with compound **2** and **6**.

In order to further establish structure-property relationship for this novel series of phosphepine-based  $\pi$ -conjugated systems **2-8**, their UV-Vis absorption and fluorescence spectra were measured both in CH<sub>2</sub>Cl<sub>2</sub> (Figure 3) and their cyclic voltammetry was measured in CH<sub>2</sub>Cl<sub>2</sub> with Bu<sub>4</sub>NPF<sub>6</sub> as electrolyte (Table 1). Furthermore, Kohn-

Sham orbitals were calculated for both conformers, together with, TD-DFT calculated vertical excitation energies (Table S3-S6).

The UV-Vis absorption spectrum of the dithieno[*b,f*]oxophosphepine **2** (Figure 3) consists of a band with an absorption maximum centered at  $\lambda_{\text{abs}} = 347$  nm. This absorption was attributed by TD-DFT calculations to a  $\pi$ - $\pi^*$  transition involving the HOMO and the LUMO (Table S8-S10). These orbitals are delocalized despite the non-planarity, and are mainly located on the  $\pi$ -conjugated backbone with a limited contribution of the P-atom. After excitation at 347 nm, the dithieno[*b,f*]oxophosphepine **2** presents a blue emission centered at 423 nm with a low quantum yield ( $\phi = 0.06$ ) (Figure 3). **2** is also redox active, presenting a reversible reduction at relatively low potential ( $E_{\text{red}} = -2.14$  V vs Fc) and an irreversible oxidation ( $E_{\text{ox}} = +1.12$  V vs Fc) (Table 1). The extension of the  $\pi$ -conjugated system on the  $\alpha$ -positions of the thienyl moieties by a phenyl substituent (**5**) leads to a significant bathochromic shift of all optical features (Figure 3 and Table 1) and also a decrease of both redox potentials (Table 1). Accordingly, LUMO and HOMO levels decrease and increase, respectively. While the  $\pi$ -type FMOs of **5** (Figure 4) have dominant contribution from the central dithieno[*b,f*]oxophosphepine unit, the phenyl groups also contribute. Indeed, the introduction of electron-donating groups cathodically shifts the oxidation wave ( $E_{\text{ox}}^{\circ} = +0.48$  V vs. Fc<sup>+/</sup>Fc for **6**) while the introduction of electron withdrawing group shifts the reduction wave anodically ( $E_{\text{red}}^{\circ} = -1.45$  V vs. Fc<sup>+/</sup>Fc for **4**) (Table 1). In accordance, the introduction of electron-withdrawing groups such in **4** mainly affects the LUMO with density on the nitrophenyl parts, while electron rich diphenylaminophenyl substituents of **6** mainly affects the HOMO (Figure 4). Also the red shift observed in UV-Vis absorption of **5** further increases both with electro-withdrawing (**3** and **4**) and electro-donating groups (**6**) at the *para* position of both phenyl rings (Scheme 1). This is in agreement with the TD DFT calculated vertical excitation energies (Table S3-S4), which remain HOMO-LUMO  $\pi$ - $\pi^*$  transitions. Due to the nature of the FMOs in **4** and **6** (see the orbitals in Figure 4), this transition has a large charge transfer (CT) character, as is also shown by the increased relative intensity of the absorption band as well as the oscillator strength (Figure 3 and Tables S3, S4, S6). Furthermore, **6** displays solvatochromic behavior which is very weak in absorption and somewhat larger in emission, as usually observed for such quadrupolar D- $\pi$ -A- $\pi$ -D -systems (Figure S8).<sup>15</sup> The high photoluminescence quantum yield of the non-planar structures (Table 1) can be explained by the high transition probability. Even though, based on CAM-B3LYP excited state geometry optimizations (Figure S23) the  $\pi$ -system of all molecules become more planar in the excited state than in the ground state, and this increased rigidity may contribute to the emission properties.

Table 1. Photophysical and electrochemical data.

	$\lambda_{\text{abs}}^a$ [nm]	$\epsilon^a$ [M <sup>-1</sup> cm <sup>-1</sup> ]	$\lambda_{\text{em}}^a$ [nm]	$\Phi^b$ (%)	$E_{\text{ox}}^c$ [V]	$E_{\text{red}}^c$ [V]
<b>2</b>	347	13600	424	6	+1.12	-2.14 <sup>d</sup>
<b>3</b>	410	32300	473	13	+1.09	-1.74 <sup>d</sup>
<b>4</b>	425	35600	525	17	-	-1.45 <sup>d</sup>
<b>5</b>	402	27400	468	8	+0.93	-1.99 <sup>d</sup>
<b>6</b>	454	41400	580	30	+0.48 <sup>d</sup>	-1.99 <sup>d</sup>
<b>8</b>	459	30100	575	0.4	+0.51 <sup>d</sup>	-1.49 <sup>d</sup>

<sup>a</sup>In CH<sub>2</sub>Cl<sub>2</sub> (10<sup>-5</sup>M). <sup>b</sup>Measured relative to quinine sulfate (H<sub>2</sub>SO<sub>4</sub>, 1 N),  $\phi_{\text{ref}} = 0.546$ . <sup>c</sup>In CH<sub>2</sub>Cl<sub>2</sub> with Bu<sub>4</sub>N<sup>+</sup>PF<sub>6</sub><sup>-</sup> (0.2 M) at a scan rate of 100 mVs<sup>-1</sup>.  $E_{\text{ox}}^{\circ}$  ( $E_{\text{red}}^{\circ}$ ) = 1/2( $E_{\text{pc}}$  +  $E_{\text{pa}}$ ) for reversible or quasi-reversible process, otherwise  $E_{\text{ox}}^{\circ}$  ( $E_{\text{red}}^{\circ}$ ) = ( $E_{\text{pa}}$ ). Potentials vs ferrocene/ferrocenium. <sup>d</sup>quasi-reversible process.

For the asymmetric compound **8**, both oxidation *and* reduction potentials are lowered with respect to **5**, in accordance with the DFT

calculated FMOs, which are located mainly on the triphenylamine (HOMO), or nitrophenyl (LUMO) part of the molecule. This suggests that the HOMO-LUMO excitation should exhibit at even higher bathochromic shift than for **4** or **6**, and also the intensity should further increase together with the even larger CT character of the transition. Surprisingly, both absorption and emission maxima for **8** match closely with the ones of symmetric **6**, and the solvatochromic behavior is also similar (Figure S9). Furthermore, the intensities are reduced, indicating *less* charge transfer than for the symmetric **6**! Both of these experimental findings are in accordance with the calculated transition energies and oscillator strengths in case of most functionals used (but not B3LYP – see SI). Unlike for **2-6**, the lowest energy transition of **8** is *not* dominated by the HOMO-LUMO excitation, but also HOMO-1 – LUMO has a significant weight. B3LYP, which gives rather accurate excitation energies for **2-6**, fails to describe this aspect resulting in a bad performance in case of **8**.<sup>16</sup>

These data show that the introduction of lateral  $\pi$ -substituents on the dithieno[*b,f*]oxophosphepine backbone allows fine tuning of the absorption/emission in the visible range and also the redox properties, despite the non-planarity of the system. In particular, compound **6** displays a straightforward synthesis and ambiphilic redox character with reversible electrochemical waves (Table 1) making it appealing for application in optoelectronic devices.

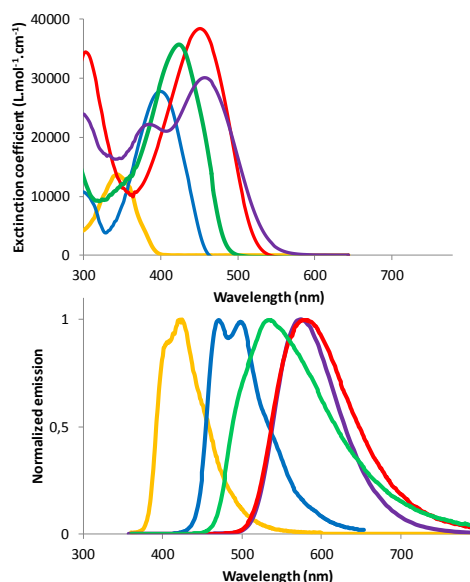


Figure 3. UV-vis absorption (up) and emission (down) of **2** (yellow), **5** (blue), **4** (green), **6** (red) and **8** (purple) in diluted DCM.

Before using the  $\pi$ -extended phosphepines as active material in devices, we investigated their thermal stability because some phosphepines are known to be rather unstable.<sup>17</sup> An intramolecular ring closure leading to the formation of phosphanorcaradiene and to a release of phosphinidene can take place. However, this transformation is usually blocked by the introduction of  $\alpha$ -*t*-Bu substituents,<sup>18</sup> or by benzannellation.<sup>17</sup> The thermogravimetric analyses (TGA) measurements performed on compound **6** show a decomposition temperature at 10% weight loss ( $T_{d10}$ ) of 400 °C (Figure S20). Furthermore, differential scanning calorimetry (DSC) measurements show no melting point. Repeat-

ing heating up to 350°C and cooling to 30°C resulted in no crystallization or melting behaviors (Figure S21). These results indicate that compound **6** presents good morphological and thermal stability. Finally, Bottom-Gate Bottom-Contact OFETs were realized by sublimation of the compound **6** and were electrically characterized under nitrogen atmosphere with an Keithley 2636A parameter analyzer, yielding moderate performance (on-/off-current ratio  $I_{on}/I_{off} = 8.8 \cdot 10^5$ , field-effect mobilities on the order of  $10^{-6} \text{ cm}^2/\text{Vs}$ , threshold voltage  $V \approx -48 \text{ V}$ ). These data seem to show the presence of a high density of defects in the first layers of the semiconductor. These problems will be addressed in the future by studying the effect of substrate temperature during sublimation step. If grain size is improved, defect density in the film will decrease leading to better electrical performances of the device. This first result shows that  $\pi$ -extended phosphepines can be suitable semiconductors for OFETs.

In conclusion, the synthesis of a new family of  $\pi$ -extended phosphepines **2-8** has been described. The Pd-catalyzed direct-arylation allows the introduction of various substituents, which tunes the absorption/emission in the visible range as well as the redox properties. All those modifications were rationalized through theoretical calculations (DFT). Finally, compound **6** could be introduced into p-type OFET. This novel P-heterocycle thus appears as a promising tunable building block for application in optoelectronics.

## ASSOCIATED CONTENT

### Supporting Information

Synthetic procedure, complete characterizations, X-ray crystallographic data and CIF files, computational details. The Supporting Information is available free of charge on the ACS Publications website.

## AUTHOR INFORMATION

### Corresponding Author

\*E-mail: zbenko@mail.bme.hu

\*E-mail: nyulaszi@mail.bme.hu

\*E-mail: pierre-antoine.bouit@univ-rennes1.fr

\*E-mail: muriel.hissler@univ-rennes1.fr

### ORCID

Muriel Hissler : 0000-0003-1992-1814

Pierre-Antoine Bouit: 0000-0002-0538-9276

Thierry Roisnel: 0000-0002-6088-4472

László Nyulászi: 0000-0002-2207-8410

### Notes

The authors declare no competing financial interest

## ACKNOWLEDGMENT

This work is supported by the Ministère de la Recherche et de l'Enseignement Supérieur, the CNRS, the Région Bretagne, Balaton PHC (38522ZH), the French National Research Agency (ANR Heterographene ANR-16-CE05-0003-01, ANR Fluohyb - ANR-17-CE09-0020), OTKA NN 113772 and BME-Nanonotechnology FIKP grant of EMMI (BME FIKP-NAT) for LN, and COST CM10302 (SIPS), PICS SmartPAH (08062).



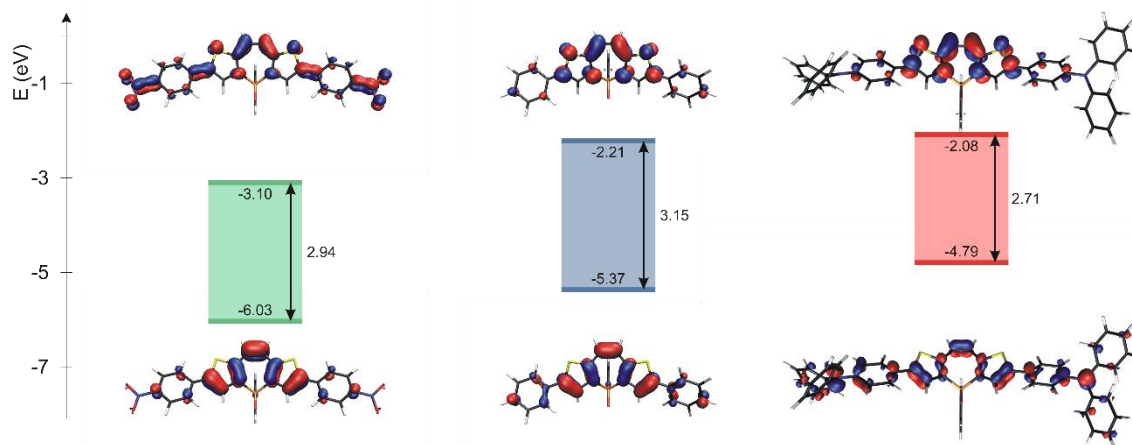


Figure 4: FMOs of **4**, **5** and **6** at the B3LYP/6-31+G\* level

## REFERENCES

- <sup>1</sup> K. Müllen, U. Scherf, (Eds.), *Organic Light Emitting Devices: Synthesis Properties and Applications*, Wiley-VCH, Weinheim, Germany **2006**
- <sup>2</sup> Roncali, J. Synthetic Principles for Bandgap Control in Linear  $\pi$ -Conjugated Systems, *Chem. Rev.* **1997**, 97, 173.
- <sup>3</sup> (a) Hissler, M.; Dyer, P. W.; Réau, R., Linear organic  $\pi$ -conjugated systems featuring the heavy Group 14 and 15 elements. *Coord. Chem. Rev.* **2003**, 244, 1-44. (b) T. Baumgartner, F. Jaekle, (Eds), Main Group Strategies toward Functional Hybrid Materials, **2018**, John Wiley & Sons (UK)
- <sup>4</sup> (a) Joly, D.; Bouit, P. A.; Hissler, M., Organophosphorus derivatives for electronic devices. *J. Mater. Chem. C* **2016**, 4, 3686-3698. (b) Stolar, M.; Baumgartner, T., Phosphorus-Containing Materials for Organic Electronics. *Chem. – As. J.* **2014**, 9, 1212-1225.
- <sup>5</sup> Chen, H.; Pascal, S.; Wang, Z.; Bouit, P.-A.; Wang, Z.; Zhang, Y.; Tondelier, D.; Geffroy, B.; Réau, R.; Mathey, F.; Duan, Z.; Hissler, M., 1,2-Dihydrophosphite: A Platform for the Molecular Engineering of Electroluminescent Phosphorus Materials for Light-Emitting Devices. *Chem. Eur. J.* **2014**, 20, 9784-9793.
- <sup>6</sup> (a) Duffy, M. P.; Delaunay, W.; Bouit, P. A.; Hissler, M.,  $\pi$ -Conjugated phospholes and their incorporation into devices: components with a great deal of potential. *Chem. Soc. Rev.* **2016**, 45, 5296-5310; (b) Ren, Y.; T. Baumgartner, Combining form with function – the dawn of phosphole-based functional materials. *Dalton Trans.* **2012**, 41, 7792-7800.
- <sup>7</sup> (a) Müller, C.; Broeckx, L. E. E.; de Krom, I.; Weemers, J. J. M., Developments in the Coordination Chemistry of Phosphinines. *Eur. J. Inorg. Chem.* **2013**, 201, 187-202. (b) Regulska, E.; Romero-Nieto, C., Highlights on  $\pi$ -systems based on six-membered phosphorus heterocycles. *Dalton Trans.* **2018**, 47, 10344-10359.
- <sup>8</sup> a) Lyaskovskyy, V.; van Dijk-Moes, R. J. A.; Burck, S.; Dzik, W. I.; Lutz, M.; Ehlers, A. W.; Slootweg, J. C.; de Bruin, B.; Lammertsma, K., Dibenzo[b,f]phosphepines: Novel Phosphane–Olefin Ligands for Transition Metals. *Organometallics* **2013**, 32, 363-373. (b) He, X.; Borau-Garcia, J.; Woo, A. Y. Y.; Trudel, S.; Baumgartner, T., Dithieno[3,2-c:2',3'-e]-2,7-diketophosphepin: A Unique Building Block for Multifunctional  $\pi$ -Conjugated Materials. *J. Am. Chem. Soc.* **2013**, 135, 1137-1147. (c) Ren, Y.; Sezen, M.; Guo, F.; Jäkle, F.; Loo, Y.-L., [d]-Carbon–carbon double bond engineering in diazaphosphepines: a pathway to modulate the chemical and electronic structures of heteropines. *Chem. Sci.* **2016**, 7, 4211-4219. (d) Winter, W., Darstellung und Stereochemie von 1,2,3,4,9-Pentaphenyl-9H-tribenzo[b,d,f]phosphshepin, *Chem. Ber* **1976**, 109, 1405-2419.
- <sup>9</sup> Stolar, M.; Reus, C.; Baumgartner, T., Xylene-Bridged Phosphaviologen Oligomers and Polymers as High-Performance Electrode-Modifiers for Li-Ion Batteries. *Adv. Ener. Mater.* **2016**, 6, 1600944.
- <sup>10</sup> Levine, D. R.; Siegler, M. A.; Tovar, J. D., Thiophene-Fused Borepins As Directly Functionalizable Boron-Containing  $\pi$ -Electron Systems. *J. Am. Chem. Soc.* **2014**, 136, 7132-7139.
- <sup>11</sup> Similar procedure was also used in reference 8a
- <sup>12</sup> Schipper, D. J.; Fagnou, K. Direct Arylation as a Synthetic Tool for the Synthesis of Thiophene-Based Organic Electronic Materials. *Chem. Mater.* **2011**, 23, 1594-1600.
- <sup>13</sup> (a) Lafrance, M.; Fagnou, K., Palladium-Catalyzed Benzene Arylation: Incorporation of Catalytic Pivalic Acid as a Proton Shuttle and a Key Element in Catalyst Design. *J. Am. Chem. Soc.* **2006**, 128, 16496-16497; (b) Liu, S.-Y.; Shi, M.-M.; Huang, J.-C.; Jin, Z.-N.; Hu, X.-L.; Pan, J.-Y.; Li, H.-Y.; Jen, A. K. Y.; Chen, H.-Z. C–H activation: making diketopyrrolopyrrole derivatives easily accessible. *J. Mater. Chem. A* **2013**, 1, 2795-2805.
- <sup>14</sup> Even if the reaction proceeds in the “classical conditions” for **4**, better yields were obtained using ligand and additives.
- <sup>15</sup> Dereka, B.; Rosspeintner, A.; Li, Z.; Liska, R.; Vauthey, E., Direct Visualization of Excited-State Symmetry Breaking Using Ultrafast Time-Resolved Infrared Spectroscopy, *J. Am. Chem. Soc.* **2016**, 138, 4643–4649.
- <sup>16</sup> Laurent, A. D.; Jacquemin, D., TD-DFT Benchmarks: A Review. *Int. J. Quantum Chem.*, **2013**, 113, 2019-2039
- <sup>17</sup> Borst, M. L. G.; Buló, R. E.; Gibney, D. J.; Alem, Y.; de Kanter, F. J. J.; Ehlers, A. W.; Schakel, M.; Lutz, M.; Spek, A. L.; Lammertsma, K., 3H-Benzophosphepine Complexes: Versatile Phosphinidene Precursors. *J. Am. Chem. Soc.* **2005**, 127, 16985-16999.
- <sup>18</sup> Märkl, G.; Burger, W. 2,7-Di-tert-butyl-1-phenyl-1H-phosphepine-The First Stable, Monocyclic Phosphepine *Angew. Chem., Int. Ed. Engl.* **1984**, 23, 894–895.